SSRG International Journal of Electronics and Communication Engineering
ISSN: 2348-8549/ https://doi.org/10.14445/23488549/IJECE-V11I8P122

Volume 11 Issue 8, 218-226, August 2024


*Original Article*

# Modelling of Optimized Conformal Antenna Array for Airborne Applications

B. R. Pushpa[1], P. V. Pushpa[2], Devaraju Ramakrishna[3]

[1,2]*Department of Electronics and Communication Engineering, Dayananda Sagar University, Karnataka, India.*
[3]*Department of Electronics and Telecommunication Engineering, Dayananda Sagar College of Engineering, Karnataka, India*.

[1]*Corresponding Author : pushpa-tce@dayanandasagar.edu*

Received: 16 June 2024 Revised: 29 July 2024 Accepted: 14 August 2024 Published: 31 August 2024

***Abstract*** *- The design and synthesis of conformal array antennas that are optimized in terms of gain, VSWR, efficiency and other antenna performance parameters, specifically for airborne applications, has been a challenging task for scientists and researchers. In this paper, a novel approach to the design, simulation and fabrication of a 1x4 microstrip patch antenna array with two Wilkinson 3-dB power dividers on FR-4 substrate is presented. The resonance frequencies chosen are 3.6 GHz for uplink and 3.4 GHz for downlink in the n78 band of 5G NR (New Radio) communication in India. The 1x4 array is designed to be simulated, and synthesis results are obtained for planar and curved surfaces to achieve conformability. The different curvatures implemented are circular-bend and U-shaped bends for the fabricated antenna array. This high degree of flexibility for testing purposes and excellent dimensional stability is offered by the dielectric material FR-4 laminate 6150/6150C. The inset feeding technique is used to feed power to the antenna array, which is not only simple but also offers good impedance matching between the terminals. The software tool used for simulation is CST (Computer Simulation Technology) Studio Suite. The proposed antenna array gives a phenomenal gain of 13.6 dB (for both uplink and downlink frequencies), HPBW of 75.9° and SLL of -11.5dB, all of which are the optimum values obtained from its previous counterparts (single patch and 1x2 array designed and simulated for the same frequencies. These results have also been found to be better than those of any contemporary designs and variants. The proposed array finds applications in drones, military spacecrafts, point-to-point communication links (because of narrow bandwidth) and air traffic control and management systems.*

***Keywords*** *- Airborne, Conformal antennas, Downlink, fabrication, Substrate.*

## 1. Introduction

Conformal antenna arrays have been extensively used in military and civilian applications because of the advantages they offer over their planar counterparts, like conformability to the shape of the surface on which they are mounted, availability in various curvatures and sizes and coverage of nearly 360°. However, the design and fabrication of optimized conformal arrays for airborne applications is a challenging task as trade-offs between various antenna performance parameters are involved. The key observations made from the survey of relevant literature from [3-10] reveal that the highest gain achieved is 11.35dBi at 35GHz. Most of the research is done in mmWave bands, which are very high-frequency bands of 5G NR communications in India. Also, the dielectric substrate material used for simulation and fabrication is expensive and complex. This research paper presents a novel approach to the design, simulation and fabrication of a microstrip patch 1x4 antenna array for the frequencies of 3.6 GHz for uplink and 3.4 GHz for downlink in a typical 5G NR n78 band of India. The proposed antenna structure is simple to design, offers good impedance matching between the antenna feed lines because of the inset feed technique employed, has a high degree of conformability to the surface on which it is mounted because of the excellent dielectric material used and shows a phenomenal gain of 13.6 dB for both uplink and downlink frequencies. Further, the antenna does not make use of any slots or complex geometrical structures to enhance the performance parameters of the antenna array, which may make it difficult to fabricate and test the units in appropriate environments [15].

The substrate used here for simulation and fabrication is FR-4 with a dielectric constant of 4.4, loss tangent of 0.018 and thickness of 0.2 mm with excellent dimensional stability and high flexibility that make it suitable for testing at various curvatures as appliable for conformal applications. Important parameters of the substrate material are included in Table 1. The simulation results for the 1x4 array are obtained in terms of VSWR, return loss, impedance match, directivity, HPBW, 2D and 3D gain plots. The fabricated units are tested, and results are obtained for three categories, namely planar, circular bend and U-bend.

**Table 1. Substrate specifications**

| Parameter (Symbol) | Typical Value |
|---|---|
| Name | Conventional FR-4/Normal Tg |
| Thermal Stress (Σ) | ≥180 s |
| Glass Transition (Tg) | 132 |
| Dielectric Breakdown | ≥45 kV |
| Flammability | V-0 |
| Dielectric Constant ($\varepsilon_r$) | 4.4 |
| Loss Tangent (δ) | 0.018 |
| Surface Resistivity (ρS) | $1.0x10^6$ MΩ |
| Volume Resistivity (ρ) | $1.0x10^8$ MΩcm$^{-1}$ |
| Arc Resistance | 125 s |
| Flexural Strength (σ) | 440 N/mm$^2$ |
| Moisture Absorption | 0.19% |

The dielectric material used is flame resistant-4 laminate 6150/6150C with specifications as summarized in Table 1. It has excellent heat and moisture resistance and dependable dimensional stability.

The characteristic that contributes to this exceptional feature of the substrate is the epoxy resin used during fabrication, which has high thermal and chemical resistance. It has other advantages over conventional materials like high thermal conductivity, low smoke generation, good insulation performance and superior heat dissipation preference.

The dielectric material used has the following features and advantages over conventional materials or meta-materials normally employed for conformal arrays [25]. The excellent dimensional stability and heat resistance offered by FR-4 material makes it suitable for aerospace applications. It offers high thermal conductivity, low smoke generation and good insulation performance, making it ideal for high-voltage applications. The unique molecular structure of the dielectric substrate used allows for uniform thickness throughout the structure, making it easy to fold, wrap, and transport.

## 2. Design

The design of a 1x4 array with two 3-dB Wilkinson power dividers, as shown in Figure 1, involves an inset feed for the array. The various parameters under consideration for design are: operating frequency, also called as the resonant frequency, which is chosen to be 3.6 GHz as uplink and 3.4 GHz as downlink frequencies; types of polarization, namely Linear Polarization (LP) and Cross-Polarization (CP); impedance matching to be achieved is for 50Ω according to standard in India; configuration of the array is conformal; the substrate material taken is FR-4 having a dielectric constant 4.4; type of power feed technique is the inset feed to achieve optimum impedance match between feed lines and the array; dimensions of the array that comprises of its geometry, dimensions of power dividers employed and the interelement spacing.

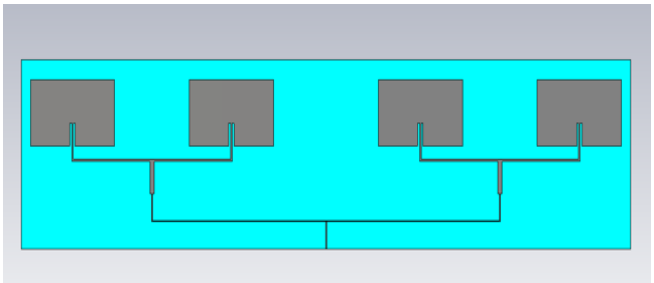

**Fig. 1 Design layout of 1x4 array for both uplink and downlink**

The basic layout for placing the four rectangular microstrip patches and two 3dB Wilkinson power dividers is as shown in Figure 1. The detailed design procedures and dimensions are explained in further sections.

### *2.1. 1x4 Array Design*

The design of any array comprises the calculation of a significant parameter called effective refractive index $\varepsilon_{eff}$. Radiations from microstrip patch antenna pass through the ground and air interface in between, resulting in fringing fields. This is not desirable as it affects the radiation and has to be minimized. The refractive indices of air and the substrate are different. Hence, the dielectric constant's effective value, called "effective refractive index", has to be calculated as given by,

$$\varepsilon_{eff} = \frac{\varepsilon_r+1}{2} + \frac{\varepsilon_r-1}{2}\left[\frac{1}{1+12(h/w)}\right] \quad (1)$$

Here (w/h)>1, and 'h' indicates the height of the substrate. $\varepsilon_{eff}$ is necessary to be computed for higher operational modes of the antenna. The microstrip patch length 'L' is calculated using,

$$L = \frac{c}{2f_0\sqrt{\varepsilon_{eff}}} - 0.824h\left[\frac{\varepsilon_{eff}+0.3\left(\frac{w}{h}+0.264\right)}{\varepsilon_{eff}-0.258\left(\frac{w}{h}+0.8\right)}\right] \quad (2)$$

The fringing effect is taken into account, and the total increase in patch length, denoted by ΔL, is calculated by,

$$\Delta L = 0.5\left(\frac{c_0}{2f_r\sqrt{\varepsilon_{eff}}} - L\right) \quad (3)$$

The frequency of resonance is denoted by '$f_r$'. The width of the power feed line is calculated using the formula,

$$Z_0 = \left(\frac{60}{\sqrt{\varepsilon_{eff}}}\right)\ln\left(\frac{2h}{W}\right) \quad (4)$$

Where $Z_0$=50Ω symbolizes the characteristic impedance of a standard transmission line.

The width and length of the transmission line are calculated using the formula,

$$\frac{w}{h} = \frac{8e^4}{e^{2A}-2} \text{ for } \frac{w}{h} < 2 \quad (5)$$

The ratio of width to height is given by the following Equation if (w/h)>2.

$$\frac{w}{h} = \frac{2}{\pi}[B - 1 - \ln(2B-1) + \frac{\varepsilon_{r+1}}{2\varepsilon_r}\left\{\ln(B-1) + 0.39 - \left(\frac{0.61}{\varepsilon_r}\right)\right\}] \quad (6)$$

The constants A and B are given by the formulae,

$$A = \frac{Z_0}{60}\sqrt{\frac{\varepsilon_{r+1}}{2}} + [(\varepsilon_r - 1)(\varepsilon_r + 1)\left(0.23 + \frac{0.11}{\varepsilon_r}\right)] \quad (7)$$

$$B = \frac{377\pi}{2Z_0\sqrt{\varepsilon_r}} \quad (8)$$

## 3. Materials and Methods

### *3.1. Substrate Material*

The substrate used for fabrication of the 1x4 array is Conventional FR-4/Normal Tg KB-6150/KB-6150C with features such as excellent dimensional stability and excellent heat resistance and mechanical properties. KB-6150 is a high-quality, durable PCB with IPC-4101/D21 specification, which means that it can be used for a wide range of applications, including medical, automotive, aerospace and industrial. It has the advantages of high flame-retardant performance, excellent thermal conductivity and heat dissipation performance. It has dependable dimensional stability due to the use of epoxy resin with high thermal and chemical resistance during fabrication [28][29]. This allows the board to maintain its properties even after being exposed to high temperatures and harsh chemicals. A few important specifications of the substrate are summarized in Table 1. The unique molecular structure of its insulating material provides excellent heat and moisture resistance. Besides these, it is a highly malleable structure that can be easily bent on any curved surface for conformal applications without damaging its size, shape, or electrical or mechanical properties. The substrate thickness varies from as low as 0.05mm to as high as 3.5mm. The thickness of the PCB used in our research work for fabrication is 0.2mm. The high degree of flexibility of the material is proven by the fact that the same fabricated 1x4 array unit is conveniently bent over a circular surface and U-shaped bend, as shown in Figure 8, for testing the conformability of the antenna.

### *3.2. Microstrip Patch 1x4 Array*

The geometry of the array and layout of the 1x4 array with two 3-dB power dividers is as shown in Figures 2 and 3, for uplink and downlink, respectively, with the dimensions of the array being designed with the help of Equations from (1) to (8). The 1x4 array is designed and optimized in such a way that the parameters pertaining to a single radiating rectangular microstrip patch antenna are extended to a 1x4 array with two 3-dB power dividers and feed the power with inset feed technique as shown in figure 1. The impedance of the array and the feedline is matched to 50Ω, which is the value of the impedance of a standard microwave transmission line in India. Two 3dB Wilkinson power dividers are placed horizontally along the line to feed the four linearly placed microstrip rectangular patches with a standard interelement spacing of λ/2. The power dividers are placed at the centre of the width of rectangular patches to feed the power with equal phase and amplitude. The total dimension of PCB in terms of length and breadth is maintained constant for uplink and downlink. The only variable parameters are the length and width of individual patches and interelement spacing and width of the line connecting power dividers to the power feed port.

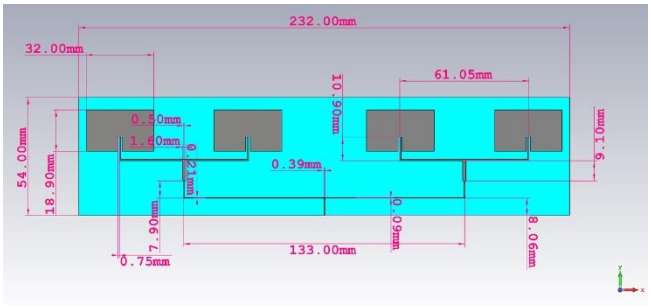


**Fig. 2 Dimensions of 1x4 array for uplink**

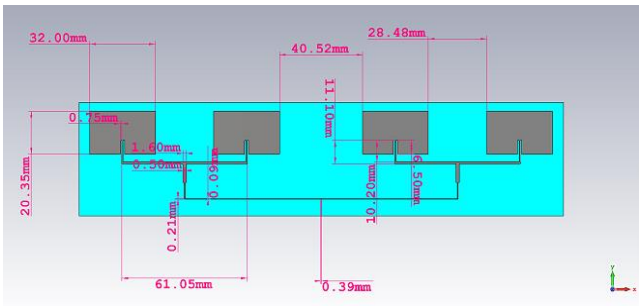


**Fig. 3 Dimensions of 1x4 array for downlink**

The lumped port for the power feed point is placed exactly at the centre of the geometry of the antenna array for equal power division between the array elements. The Wilkinson 3-dB power dividers are also placed at the centre of the length of the individual microstrip patches, as shown in Figures 2 and 3.

## 4. Results and Discussion

The results procured by simulation and post-fabrication of the 1x4 antenna array are given in the following sections. A comparison of simulation and fabrication results is also done.

### *4.1. Simulation Results*

The simulation of various antenna performance parameters like return loss, VSWR, gain, directivity, antenna impedance and bandwidth of 1x4 array for uplink 3.6 GHz and downlink 3.4 GHz is done using CST (Computer Simulation Technology) Studio Suite, version 2017.0224. The following sections detail the obtained results of the simulation.

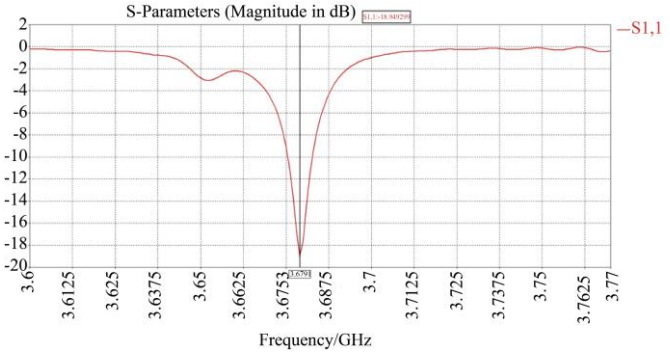


**Fig. 4 (a) S11 plot for uplink**

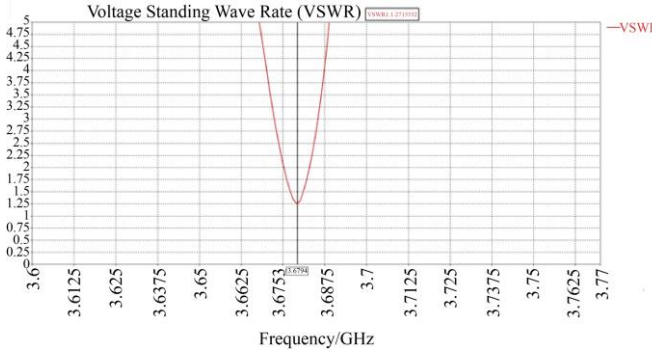


**Fig. 4 (b) Return loss of patch for uplink**

*4.1.1. Uplink 1x4 Array*

Any frequency of data or signal that is transmitted from an earth station to a satellite or, an aircraft or a base station is referred to as uplink. In a standard full-duplex communication link, it is one of the unidirectional communication channels. For the 1x4 array, the resonant frequency is found to be at 3.6791GHz, as in Figure 4(a). The array shows a return loss of -18.949dB, a fair impedance match of 46.8Ω and a far-field gain of 13.6dB, as shown in Figures 4(b), (c), (d) and (e), respectively.

The 1x4 array radiates at 3.6791GHz, which excellently matches with the frequency designed for uplink and the excellent value of $S_{11}$ of -18.949dB, as shown in Figure 4(a).

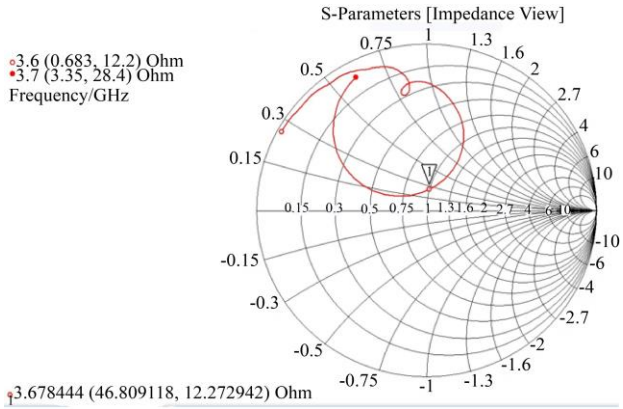


**Fig 4 (c) Impedance plot for uplink**

The array shows a good impedance match with a VSWR of 1.27, which lies in the acceptable range of 1 to 1.5, as shown in Figure 4(b).

Smith chart plot of the array, as shown in Figure 4(c), shows 46.8Ω, which is approximated to 50Ω, the standard impedance of microwave transmission line in India.

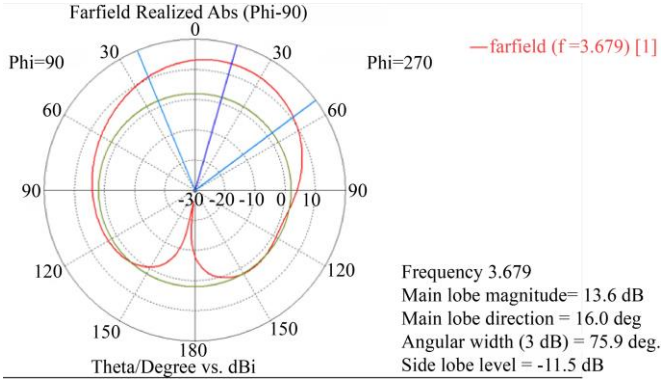


**Fig. 4 (d) 2D Farfield gain plot for uplink**

The antenna gain pattern in 2D for the 1x4 array, as shown in Figure 4(d), shows a phenomenal gain of 13.6 dB. The Side Lobe Level (SLL) is -11.5 dB.

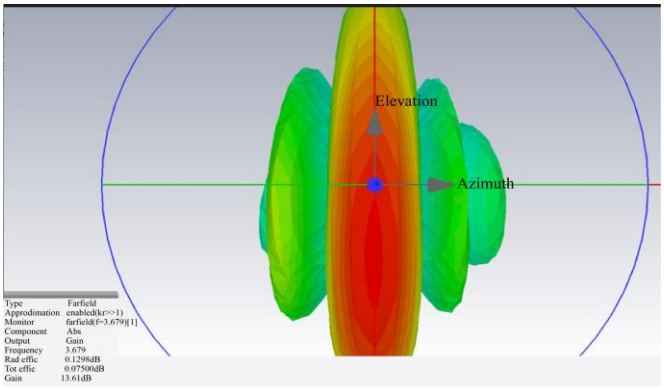


**Fig. 4 (e) 3D gain plot for uplink**

The 3D radiation plot of the array is strongest along the z-direction/azimuth angle at 13.6dB peak gain and HPBW of 75.9°, as shown in Figure 4(e).

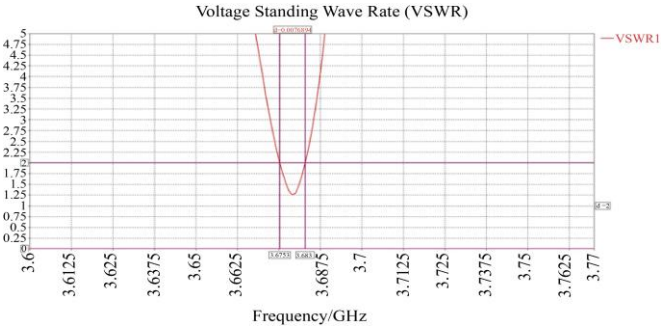


**Fig. 4 (f) 10dB BW plot for uplink**

Figure 4(f) shows the antenna BW plot measured at VSWR=2 with upper and lower cut-off frequencies of 3.683 GHz and 3.6753 GHz, respectively, giving an operational BW of 7.6894 MHz.

*4.1.2. Downlink 1x4 Array*

Any frequency of data or signal that is transmitted from a satellite or, an aircraft, or a base station to a ground station or earth station is referred to as a downlink. In a typical full-duplex communication link, it forms one of the unidirectional communication channels. The frequency of resonance for a 1x4 array is found to be at 3.425 GHz, as shown in Figure 5(a). It depicts S11 of -15.008dB, impedance matched at 63.94Ω and peak gain in the Fraunhoffer region of 13.1 dB, as shown in Figures 5(b), (c), (d) and (e), respectively.

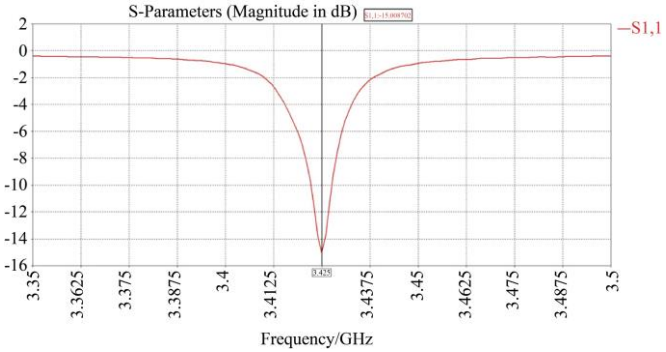


**Fig. 5 (a) S11 plot for downlink**

The 1x4 microstrip patch antenna array for downlink resonates at a frequency of 3.425 GHz, perfectly matching the designed value of 3.4 GHz. $S_{11}$ value is -15.008dB, as shown in Figure 5(a).

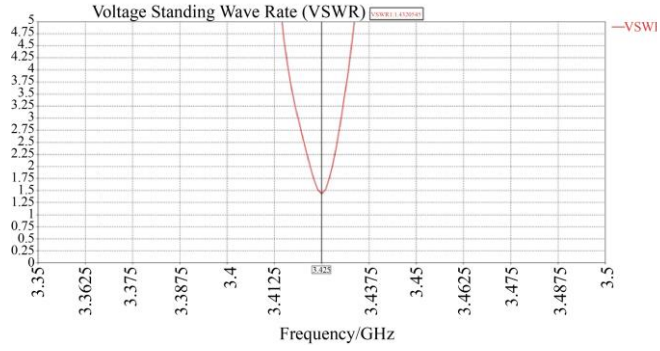


**Fig 5 (b) Return loss for downlink**

The excellent VSWR value of 1.432, which lies in the acceptable range of 1 to 1.5, is captured for downlink as known from Figure 5(b).

Smith Chart plot of Figure 5(c) indicates impedance matching at 63.94Ω and 1.4 VSWR. The impedance can be matched to standard value by using suitable stubs.

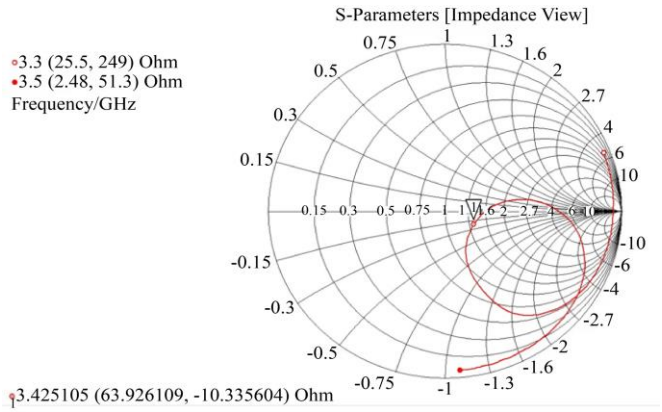


**Fig. 5 (c) Impedance plot for downlink**

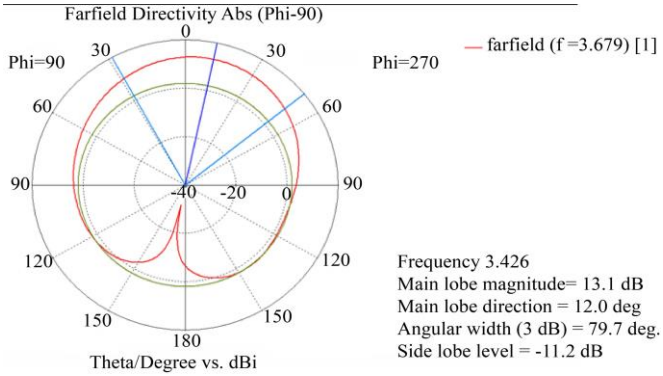


**Fig. 5 (d) 2D Farfield gain plot for downlink**

The antenna gain pattern in 2D for the 1x4 array, as seen in Figure 5(d), shows a phenomenal gain of 13.22 dB. Side Lobe Level (SLL) is -11.1dB. It is an end-fire pattern since the main lobe is oriented along 0°.

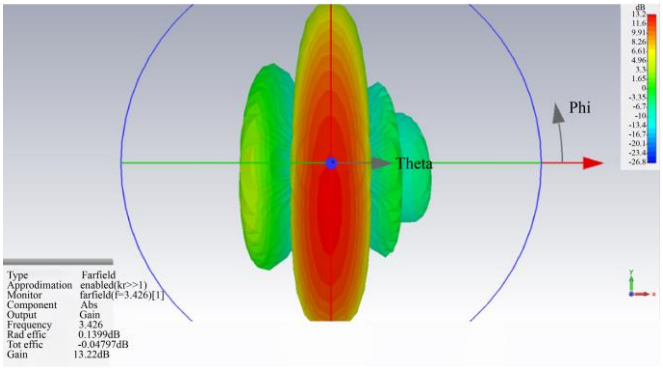


**Fig. 5(e) 3D gain plot of patch for downlink**

The gain pattern in 3D for the 1x4 array has a peak gain of 13.1dB and HPBW of 79.7°, as shown in Figure 5(e).

Figure 5(f) shows the antenna BW plot measured at VSWR=2 with an upper cut-off frequency of 3.4279 GHz and a lower cut-off frequency of 3.4219 GHz, giving an operational BW of 6.082 MHz.

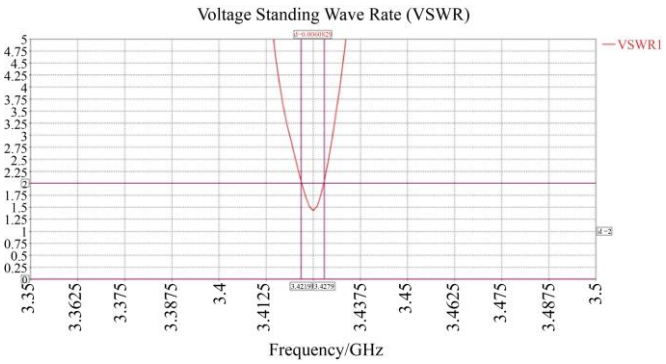


**Fig. 5(f) 10dB BW plot for downlink**

**Fig. 6 Fabricated units of single patch, 1x2 array and 1x4 array**

### *4.2. Fabrication Results*

The fabrication of a 1x4 array for both uplink and downlink frequencies is done using the FR-4 material, the specifications of which are given in Table 1. The units are shown in Figure 6 with a single radiating element at the designed resonant frequency, 1x2 array and 1x4 arrays. The testing is done in an anechoic chamber, as shown in Figure 7. The readings taken for the 1x4 antenna array fall into three categories, namely planar array (without any bending), circular array (with bending along a circular contour) and U-bend (free ends of antenna array tied to form a U-shaped bend) as shown in Figure 8. A standard 50Ω SMA connector is used to connect the feed line to the power supply.

The model of the fabricated units remains the same for both uplink and downlink, as shown in Figure 6, except for the changes in the dimensions of the patches constituting the array and interelement spacing, as summarized in Table 3.

The anechoic chamber is as shown in Figure 7 with outer dimensions 10ftx12ft. The distance of separation between the transmitting standard horn antenna mounted in the chamber and the rotatable receiver antenna table is around 7ft. The transmitter in the anechoic chamber is a standard ridged horn antenna with a length of 279mm, width of 310mm, height of 227mm and weight of 2.5kg (max). Taking this as the reference, the antenna performance parameters of the fabricated antenna are measured by mounting it on the rotating table, as shown in Figure 7.

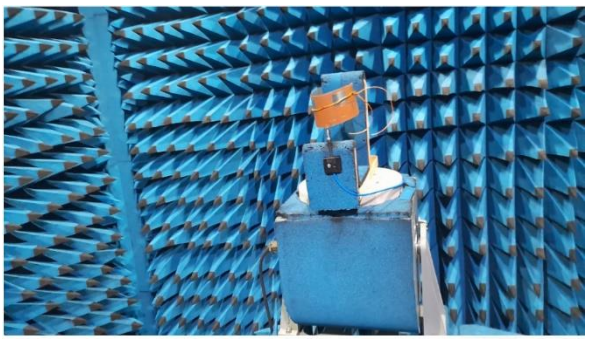

**Fig. 7 Anechoic chamber mount**

**Fig. 8 U-bend and circular bend 1x4 array**

Conformability analysis is done by giving the fabricated units with different radii of curvature to suit any application. The unit is bent over a cylindrical surface, as shown in Figure 8, to give it a circular bend and the unit is tested for various performance parameters. Also, the unit is bent, and the free ends are tied to make it a U-shaped bend. The free ends of the unit are tied using a plastic wire so that the U-shape remains intact and the wire also does not interfere with the radiation pattern of the antenna. The readings from the anechoic chamber are taken with a step-size of 10° for measuring $S_{11}$ and $S_{21}$ for both uplink and downlink. The material FR-4 proves to have a high degree of flexibility in the way it is bent over a curved surface, as shown in Figure 8. The details of the parameters obtained after design, simulation, fabrication, and testing are tabulated in Table 3 for the planar 1x4 array. A couple of sample plots of testing post-fabrication are shown in Figures 9 and 10**.** The testing of return loss or S11 of the planar 1x4 array from the anechoic chamber is shown in Figure 10.

The plot of return loss for a 1x4 circular array from an anechoic chamber post-fabrication is shown in Figure 9.

The plot of return loss for the U-bend 1x4 array from the anechoic chamber post-fabrication is shown in Figure 10.

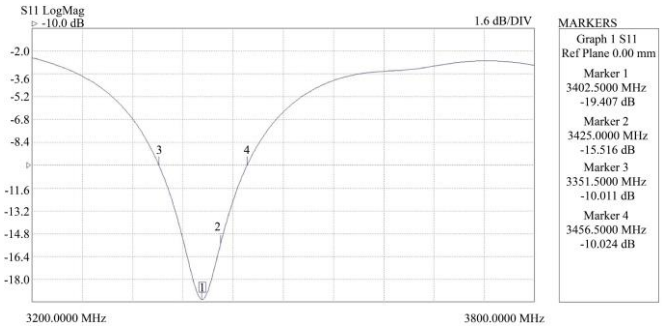


**Fig. 9 $S_{11}$ of 1x4 circular array**

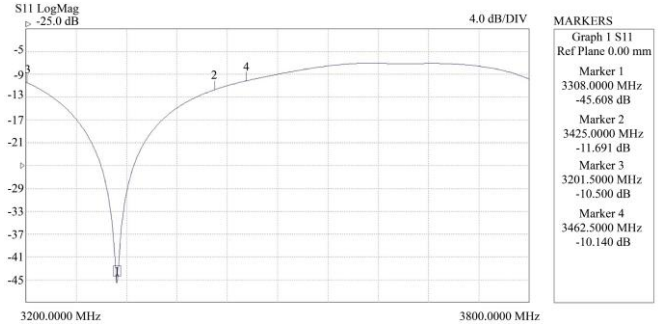


**Fig. 10 $S_{11}$ of 1x4 U-bend array**

**Table 2. Simulation and fabrication parameters of planar 1x4 array**

| Parameter | Simulation | | Fabrication | |
|---|---|---|---|---|
| | Uplink | Downlink | Uplink | Downlink |
| Frequency of resonance (GHz) | 3.675 | 3.417 | 3.678 | 3.425 |
| VSWR | 1.27 | 1.432 | 1.37 | 1.151 |
| Impedance Match (Ω) | 46.8 | 63.94 | 49.973 | 46.706 |
| Return loss $S_{11}$ (dB) | -18.0685 | -15.008 | -17.926 | -41.4720 |
| Gain (dB) | 13.61 | 13.22 | 16.36 | 16.05 |

The designed, simulated parameters of the planar 1x4 array match those obtained after fabrication and testing in anechoic chambers, as summarized in Table 2. It can also be noted that the impedance matching has improved post-fabrication. Further, the test conformability of the antenna is tested for a couple of bending angles, as shown in Figure 9, and the results are tabulated in Table 3.

**Table 3. Fabrication-testing parameters for circular and U-bend 1x4 array**

| Parameter | Circular Array | | U-bend Array | |
|---|---|---|---|---|
| | Uplink | Downlink | Uplink | Downlink |
| Frequency of resonance (GHz) | 3.689 | 3.402 | 3.678 | 3.425 |
| VSWR | 1.499 | 1.24 | 1.426 | 1.011 |
| Impedance Match (Ω) | 71.9 | 40.8 | 71.092 | 50.473 |
| Return loss $S_{11}$ (dB) | -21.69 | -37.3163 | -15.129 | -45.608 |
| Gain (dB) | 13.42 | 16.25 | 16.23 | 14.59 |

The impedances obtained for the circular array and U-bend array require stubs for matching the impedances with 50Ω.

## 5. Conclusion

A novel approach to the design, simulation and fabrication of optimized conformal antennas is presented in this research paper for avionics applications in the n78 band of 5G NR communication in India. Two individual antennas have been designed and fabricated for uplink and downlink frequencies. The results obtained in the simulation and fabrication of a planar 1x4 array are compared. It shows a phenomenal increase in gain of 13.1dB compared to a single radiating element or lower size (1x2) arrays.

The HPBW obtained is 75.9°, which is twice that of contemporary designs. Considerable reduction in SLL is also achieved. The method used for feeding power to the array is the inset feed technique. It gives a planar structure that is suitable for proper impedance matching between radiating elements and power feedlines. The fabricated antennas exhibit excellent conformability to circular and U-shaped surfaces, as indicated in the results. Impedance matching of nearly 50Ω is achieved by the use of stubs at the radiating elements of the array. The dielectric substrate material used is exceptional in its properties and performance, as indicated by the tables and results. Conformability analysis done by bending the fabricated array over a circle and using a U-shaped bend gives excellent performance parameters. The arrays thus designed are used for avionics applications like drones, navigation systems and air traffic-control applications.

## References

[1] Mamta Agiwal, Abhishek Roy, and Navrati Saxena, "Next Generation 5G Wireless Networks: A Comprehensive Survey," *IEEE Communications Surveys & Tutorials*, vol. 18, no. 3, pp. 1617-1655, 2016. [CrossRef] [Google Scholar] [Publisher Link]

[2] Weijia Wang et al., "High-Performance Printable 2.4 GHz Graphene-Based Antenna Using Water-Transferring Technology," *Science and Technology of Advanced Materials*, vol. 20, no. 1, pp. 870-875, 2019. [CrossRef] [Google Scholar] [Publisher Link]

[3] Lars Josefsson, and Patrik Persson, *Conformal Array Antenna Theory and Design*, Wiley-IEEE Press, pp. 1-512, 2006. [CrossRef] [Google Scholar] [Publisher Link]

[4] Yuhe Liu et al., "Cylindrical Conformal Broadband Array Antenna Based on Defective Ground Structure," *2019 IEEE 4th Advanced Information Technology, Electronic and Automation Control Conference*, Chengdu, China, pp. 382-385, 2019. [CrossRef] [Google Scholar] [Publisher Link]

[5] Nevin Altunyurt et al., "Conformal Antennas on Liquid Crystalline Polymer Based Rigid-Flex Substrates Integrated with the Front-End Module," *IEEE Transactions on Advanced Packaging*, vol. 32, no. 4, pp. 797-808, 2009. [CrossRef] [Google Scholar] [Publisher Link]

[6] J. Suganthi, T. Kavitha, and V. Ravindra, "Survey on Metamaterial Antennas," *International Conference on Recent Innovations in Engineering and Technology*, Tamil Nadu, India, vol. 1070, pp. 1-14, 2020. [CrossRef] [Google Scholar] [Publisher Link]

[7] J. Monica, and P. Jothilakshmi, "A Design of Bandwidth-Enhanced Conformal Antenna for Aircraft Applications," *IETE Journal of Research*, vol. 69, no. 1, pp. 447-459, 2023. [CrossRef] [Google Scholar] [Publisher Link]

[8] Wei Hong et al., "Multibeam Antenna Technologies for 5G Wireless Communications," *IEEE Transactions on Antennas and Propagation*, vol. 65, no. 12, pp. 6231-6249, 2017. [CrossRef] [Google Scholar] [Publisher Link]

[9] Syeda Fizzah Jilani et al., "Millimeter-Wave Liquid Crystal Polymer Based Conformal Antenna Array for 5G Applications," *IEEE Antennas and Wireless Propagation Letters*, vol. 18, no. 1, pp. 84-88, 2019. [CrossRef] [Google Scholar] [Publisher Link]

[10] Chun-Xu Mao et al., "Planar Sub-Millimeter-Wave Array Antenna with Enhanced Gain and Reduced Sidelobes for 5G Broadcast Applications," *IEEE Transactions on Antennas and Propagation*, vol. 67, no. 1, pp. 160-168, 2019. [CrossRef] [Google Scholar] [Publisher Link]

[11] Wei Lin, Richard W. Ziolkowski, and Hang Wong, "Pattern Reconfigurable Techniques for LP and CP Antennas with the Broadside and Conical Beams," *12th European Conference on Antennas and Propagation*, London, UK, pp. 1-4, 2018. [CrossRef] [Google Scholar] [Publisher Link]

[12] Wael Ali et al., "Planar Dual-Band 27/39 GHz Millimeter-Wave MIMO Antenna for 5G Applications," *Microsystem Technologies*, vol. 27, pp. 283-292, 2021. [CrossRef] [Google Scholar] [Publisher Link]

[13] T.E. Morton, and K.M. Pasala, "Pattern Synthesis of Conformal Arrays for Airborne Vehicles," *2004 IEEE Aerospace Conference Proceedings (IEEE Cat. No.04TH8720)*, Big Sky, MT, USA, vol. 2, pp. 1030-1039, 2004. [CrossRef] [Google Scholar] [Publisher Link]

[14] Jiazhi Dong et al., "A Research on Airborne Conformal Array with High Gain and Low SLL," 2*014 International Conference on Computational Intelligence and Communication Networks*, Bhopal, India, pp. 334-338, 2014. [CrossRef] [Google Scholar] [Publisher Link]

[15] Yeqin Huang, and S.T. Hsieh, "Radiation of Conformal Slot Arrays on Perfectly Conducting Super-Spheroid," *2005 IEEE International Symposium on Microwave, Antenna, Propagation and EMC Technologies for Wireless Communications*, Beijing, vol. 1, pp. 601-604, 2005. [CrossRef] [Google Scholar] [Publisher Link]

[16] L. Zou, J. Lasenby, and Z. He, "Beamforming with Distortionless Co-Polarisation for Conformal Arrays Based on Geometric Algebra," *IET Radar, Sonar and Navigation*, vol. 5, no. 8, pp. 842-853, 2011. [CrossRef] [Google Scholar] [Publisher Link]

[17] K.M. Tsui, and S.C. Chan, "Pattern Synthesis of Narrowband Conformal Arrays Using Iterative Second-Order Cone Programming," *IEEE Transactions on Antennas and Propagation*, vol. 58, no. 6, pp. 1959-1970, 2010. [CrossRef] [Google Scholar] [Publisher Link]

[18] Yan-Ying Bai et al., "A Hybrid IWO/PSO Algorithm for Pattern Synthesis of Conformal Phased Arrays," *IEEE Transactions on Antennas and Propagation*, vol. 61, no. 4, pp. 2328-2332, 2013. [CrossRef] [Google Scholar] [Publisher Link]

[19] Massimiliano Comisso, and Roberto Vescovo, "3D Power Synthesis with Reduction of Near-Field and Dynamic Range Ratio for Conformal Antenna Arrays," *IEEE Transactions on Antennas and Propagation*, vol. 59, no. 4, pp. 1164-1174, 2011. [CrossRef] [Google Scholar] [Publisher Link]

[20] Srabonty Soily, Rezaul Karim Mazumder, and Khaleda Ali, "Design and Simulation of Two Conformal Arrays with Dual Patch and Quadruple Patch Antenna Elements," *2015 IEEE Conference on Antenna Measurements & Applications*, Chiang Mai, Thailand, pp. 1-3, 2015. [CrossRef] [Google Scholar] [Publisher Link]

[21] M. Comisso, and R. Vescovo, "Fast 3D Pattern Synthesis for Conformal Antenna Arrays with Cross-Polarization Reduction," *2010 IEEE Antennas and Propagation Society International Symposium*, Toronto, ON, Canada, pp. 1-4, 2010. [CrossRef] [Google Scholar] [Publisher Link]

[22] Meysam Rasekh, and Saeid R. Seydnejad, "Design of an Adaptive Wideband Beamforming Algorithm for Conformal Arrays," *IEEE Communications Letters*, vol. 18, no. 11, pp. 1955-1958, 2014. [CrossRef] [Google Scholar] [Publisher Link]

[23] K. Woelder, and J. Granholm, "Cross-Polarization and Sidelobe Suppression in Dual Linear Polarization Antenna Arrays," *IEEE Transactions on Antennas and Propagation*, vol. 45, no. 12, pp. 1727-1740, 1997. [CrossRef] [Google Scholar] [Publisher Link]

[24] H. Schippers et al., "Conformal Phased Array with Beam Forming for Airborne Satellite Communication," *2008 International ITG Workshop on Smart Antennas*, Darmstadt, Germany, pp. 343-350, 2008. [CrossRef] [Google Scholar] [Publisher Link]

[25] Peter Knott, "Design of a Triple Patch Antenna Element for Double Curved Conformal Antenna Arrays," *2006 First European Conference on Antennas and Propagation*, Nice, France, pp. 1-4, 2006. [CrossRef] [Google Scholar] [Publisher Link]

[26] Ziheng Ding et al., "High Aperture Efficiency Arced Conformal Array with Phasor Beam Steering Antenna," *IEEE Transactions on Antennas and Propagation*, vol. 71, no. 1, pp. 596-605, 2023. [CrossRef] [Google Scholar] [Publisher Link]

[27] Fujun Xu et al., "Performance and Impact Damage of a Three Dimensionally Integrated Microstrip Feeding Antenna Structure," *Composite Structures*, vol. 93, no. 1, pp. 193-197, 2010. [CrossRef] [Google Scholar] [Publisher Link]

[28] Lan Yao et al., "Fabrication and Impact Performance of Three-Dimensionally Integrated Microstrip Antennas with Microstrip and Coaxial Feeding," *Smart Materials and Structures*, vol. 18, no. 9, 2009. [CrossRef] [Google Scholar] [Publisher Link]

[29] Brajlata Chauhan et al., "Cylindrical Conformal Antenna Arrays Theory for Military Aircraft Antenna," *2020 IEEE International Conference on Computing, Power and Communication Technologies*, Greater Noida, India, pp. 77-82, 2020. [CrossRef] [Google Scholar] [Publisher Link]

[30] Bahare Mohamadzade et al., "Recent Developments and State of the Art in Flexible and Conformal Reconfigurable Antennas," *Electronics*, vol. 9, no. 9, pp. 1-26, 2020. [CrossRef] [Google Scholar] [Publisher Link]

[31] G. Shine Let et al., "Split Ring Resonator-Based Conformal Antenna for Earth Coverage Spaceborne Applications," *Computer Aided Constellation Management and Communication Satellites Lecture Notes in Electrical Engineering*, vol. 987, pp. 9-16, 2023. [CrossRef] [Google Scholar] [Publisher Link]

[32] Neng-Wu Liu et al., "A Low-Profile Aperture-Coupled Microstrip Antenna with Enhanced Bandwidth under Dual Resonance," *IEEE Transactions on Antennas and Propagation*, vol. 65, no. 3, pp. 1055-1062, 2017. [CrossRef] [Google Scholar] [Publisher Link]

[33] Ling Sun et al., "Two-Port Pattern Diversity Antenna for 3G and 4G MIMO Indoor Applications," *IEEE Antennas and Wireless Propagation Letters*, vol. 13, pp. 1573-1576, 2014. [CrossRef] [Google Scholar] [Publisher Link]